Figure 3.1.12 Catalyst Deactivation Rates in Different Reactors

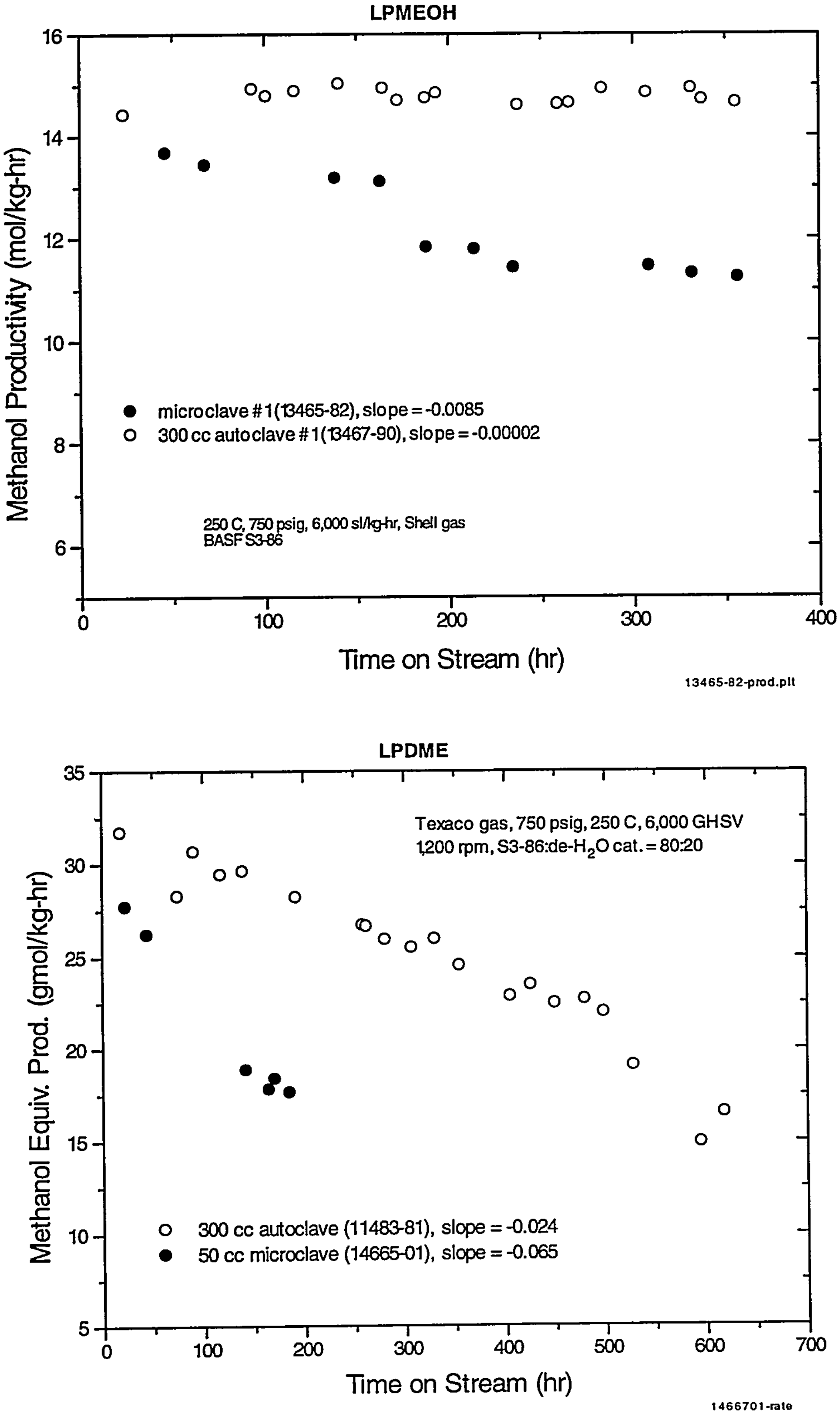

Abrasion and Attrition

Abrasion of the surface of the hardware inside the lab reactors might be the problem because this abrasion could continuously generate a new surface of stainless steel (300-cc autoclave) or Hastelloy C (50-cc microclave). This new surface might then react with CO to form iron and nickel carbonyls, which are known methanol catalyst poisons. To investigate this possibility, LPMEOH™ and LPDME™ runs were performed in a 300-cc autoclave with a copper liner inside the reactor. Little difference was observed between these runs and those without a copper liner. Mention needs to be made that other reactor internals used in these experiments, including the stirrer, dip tube, baffle blades, and thermocouple well, were made of steel, and were not shielded or replaced by benign materials.

Another way to investigate the abrasion hypothesis is to use different stirring rates, assuming that a higher stirring rate would cause more severe abrasion. Stirring could also accelerate the attrition of catalyst particles, which might then lead to faster deactivation of both methanol and dehydration catalysts because of more intimate contact between smaller particles. Since more rigorous stirring is used in smaller reactors to overcome mass transfer limitations, and since the smaller reactors have smaller volume-to-surface ratios, this theory predicts faster deactivation in smaller reactors.

To test these hypotheses, the standard catalyst mixture containing BASF S3-86 methanol catalyst and Catapal B δ-alumina was loaded into two 50-cc miniclaves. The run in miniclave #2 (14047-61) used the normal rotational speed, 2,000 rpm. A lower stirrer rate, 500 rpm, was used for the run in miniclave #1 (14667-20). However, during data acquisition, the stirrer rate in the reactor was increased to 2,000 rpm to overcome the mass transfer limitation. In total, the #1 miniclave stirrer speed was 500 rpm for 90% of the time. The two runs were carried out in parallel, sharing the same feed gas and analytical system. The results from these parallel runs are shown in Figure 3.1.13. It can be seen that the methanol catalyst deactivates in a similar manner under different stirrer rates. The deactivation of the dehydration catalyst in the two reactors is also similar (not shown). These results indicate that more rigorous stirring in smaller reactors is not responsible for the faster catalyst deactivation.

Figure 3.1.13 Methanol Catalyst Deactivation under Different Stirrer Rates

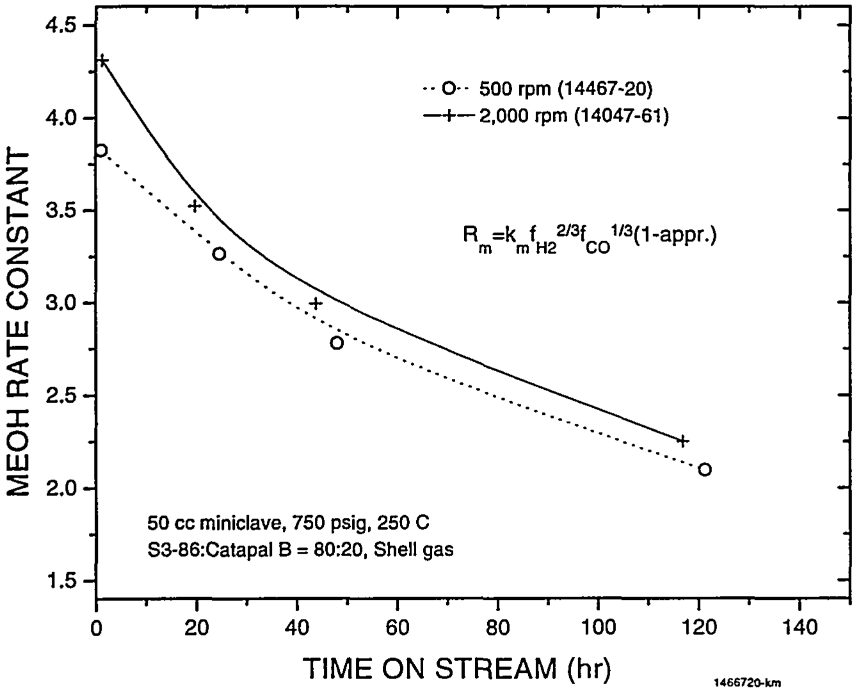

In summary, the experiments using the copper liner and different stirring rates suggest that surface abrasion of reactor internals and catalyst attrition do not play a significant role in the catalyst deactivation seen with both LPMEOH™ and LPDME™ formation; therefore, they are unlikely to be the cause of the experimental artifact.

Loss of Catalysts to the Walls of Reactor Internals

Another possible cause of deactivation related to reactors of small volume-to-surface ratios is the loss of catalyst on the reactor internals. This can be caused by the caking of catalyst powders on the walls from the decrease in slurry level during the run, or from spattering of the slurry onto the section that is not covered by the slurry. It could also be due to clumping of the catalyst powders on the buffer blade, dip tube, thermocouple well, and the shaft of the stirrer. Both the caking and clumping described above have been observed; however, the amount of caking and clumping is small, and thus do not seem to be significant enough to account for the corresponding loss in activity. This possibility is still under investigation.

Poisons from the Feed Gas

We have also investigated possible poisons to the methanol catalyst in the feed gas. This seems to be very unlikely because carbon traps are used in the feed gas line to remove carbonyls. Furthermore, little deactivation was observed in the runs using Robinson-Mahoney basket internals. If the feed gas contained poisons, methanol catalyst deactivation should have been observed in these runs. To double check on this, we conducted two LPDME™ runs in a microclave using different amounts of catalysts (by a factor of 2), but the same gas flow rate. If the artifact that causes the deactivation were due to the poisons in the feed gas, the run with a smaller amount of catalysts would have been exposed to more poisons, therefore, would shown a higher rate of deactivation. As displayed in Figure 14, the two runs have similar deactivation rates for the methanol catalyst (roughly two parallel curves). Therefore, the possible poisons from the feed gas is ruled out.

Figure 3.1.14 Methanol Catalyst Deactivation at Different Feed-to-Catalyst Ratios

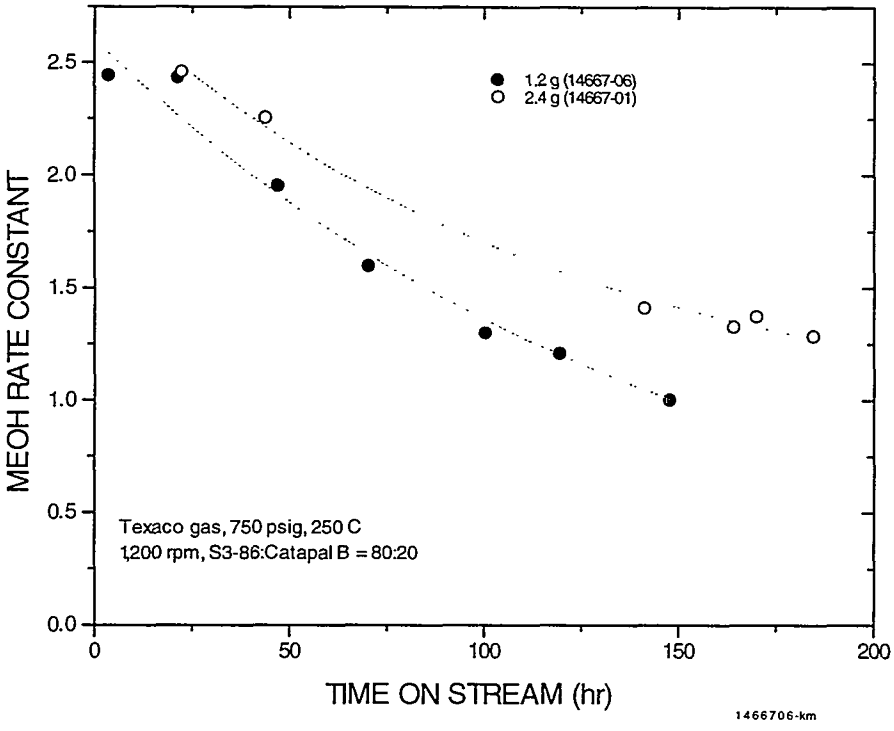

Other Metal Sulphates

Initial efforts this quarter focused on examining metal sulfates as potential methanol dehydration catalysts, working in parallel with the efforts on metal phosphates. Experiments were performed in the 50-ml microclave reactors using a 4:1 ratio of methanol synthesis catalyst (BASF S3-86) to metal sulfate, at standard reaction conditions (250°C, 750 psig, GHSV=6000 l/hr kg). Catalyst loading and stirrer speed were carefully selected to ensure that catalyst activity, not mass transfer, was rate-limiting.

Zinc sulphate, calcined at 175°C in accordance with literature data, was practically inactive for methanol dehydration, producing 0.03 gmol/hr kg of DME. Aluminum sulfate (calcined at 350°C), which has both a higher concentration of acid sites and sites of stronger acid strength, yielded 0.70 gmol/hr kg of DME. The S3-86 was relatively stable in the presence of this catalyst; methanol synthesis deactivated only slightly faster than that observed in the absence of any dehydration catalyst. However, DME productivity with the aluminum sulfate was still roughly an order of magnitude below that seen with aluminum phosphates.

One possible reason for this is the low surface area of the aluminum sulfate. To combat this problem, two approaches were tried. The first approach was supporting aluminum sulfate on a large surface area support; 12.6%$Al_2(SO_4)3/SiO_2$ was prepared by a simple aqueous impregnation on Davison Grade 58 silica gel (300 m2/g). The catalyst was then dried, ground and calcined at 350°C. Microclave testing of the resulting material demonstrated a DME productivity of 0.9 gmol/hr kg on a total catalyst weight basis; this corresponds to 7 gmol/hr kg on an aluminum sulfate basis (silica gel has been shown to have no dehydration activity). These results appear to confirm that increasing the available surface area of aluminum sulfate could bring its dehydration activity in line with that observed with aluminum phosphate. However, this supported catalyst deactivated fairly quickly and also caused rapid deactivation of the methanol synthesis catalyst.

The second approach was to prepare a larger surface area aluminum sulfate catalyst via a precipitation route, similar to that used to prepare the aluminum phosphate materials. In this approach, precipitation is initiated by the addition of base (NH_4OH) to an aqueous solution of aluminum sulfate. Although the primary product of this reaction is expected to be $[Al(H_2O)x(OH)6-x]x-3$, sulfate can "penetrate" this coordination sphere; thus, one would expect to find some degree of Al-(SO_4)-Al bonding in the final (calcined) material. This material was prepared and will be tested in late April; it will also be characterized to determine surface area and sulfate content. If this catalyst does not prove sufficiently active and stable for DME synthesis, priority will be shifted to investigating alternative metal phosphates, such as $LaPO_4$ and $GaPO_4$.

Eastman Chemical supplied five catalysts that they patented in 1993 for DME synthesis from hydrogen-rich feeds in a packed-bed reactor. These catalysts are Zn/TiO_2-based and perform both the methanol synthesis and dehydration functions at comparatively high temperatures and pressures (325°C and 1200 psig). The patented performance under these conditions was a methanol equivalent productivity of 76.8 gmol/hr kg and equimolar production of DME and methanol. We tested the most promising of these materials (based on patent data) under the patent conditions in both a packed bed reactor and the well-stirred slurry phase microclave reactor using CO-rich feed. Very poor activity and selectivity were observed in the slurry experiment (methanol equivalent productivity of 6.7 gmol/hr kg and DME/DME+MeOH of 0.30); this can be attributed at least in part to clumping of the catalyst in the slurry. The packed bed experiments did provide equimolar methanol and DME production, but the methanol equivalent productivity was still only 13.0 gmol/hr kg. Switching to a more hydrogen-rich feed slightly increased productivity, but lowered selectivity sharply (DME/DME+MeOH=0.22).

Air Products researchers observed stable activity for both methanol synthesis and dehydration when using the novel AP02 catalyst with S3-86 at 250°C; however, the system rapidly deactivated when the temperature was raised to 270°C. This raised the issue of whether our previous standard DME catalyst combination, S3-86 with Catapal-B alumina, might not be stable at slightly lower temperatures than 250°C, yet still possess reasonable catalytic activity at these temperatures since its activity at 250°C is quite high. This hypothesis was tested in the microclave under standard conditions at 220°, 230° and 240°C. These data, combined with our previous microclave data at 250°C, are shown in Figures 3.1.15 and 3.1.16. It must be noted that the rates of deactivation measured in the microclaves are typically higher than those measured in the 300-ml autoclave reactors ; in Figure 3.1.15, note the relative positions of the "S3-86" points measured in the microclave and autoclave. The Arhennius plot, Figure 3.1.16, shows that the rate constants obey a simple Arhennius law and that an increase in stability is indeed observed at lower temperatures, together with a corresponding decrease in activity. However the magnitude of this stability increase does not quite offset the activity loss when this catalyst combination is compared to the S3-86/AP02 combination (Figure 3.1.15). The ratio of S3-86 to Catapal-B has not been adjusted to optimize productivity at 230°C, as is evidenced by the high DME/methanol ratio that resulted (>2). Given these results, we may pursue a 300-ml autoclave run using the S3-86 with Catapal-B at 230°C to obtain directly comparable activity and catalyst stability data that will provide a clear "baseline" for evaluation of our improved dehydration catalysts.

Figure 3.1.15 Comparison of DME Catalyst Systems. LPMEOH™ Data from Microclave and Autoclave Reactors provided for comparison

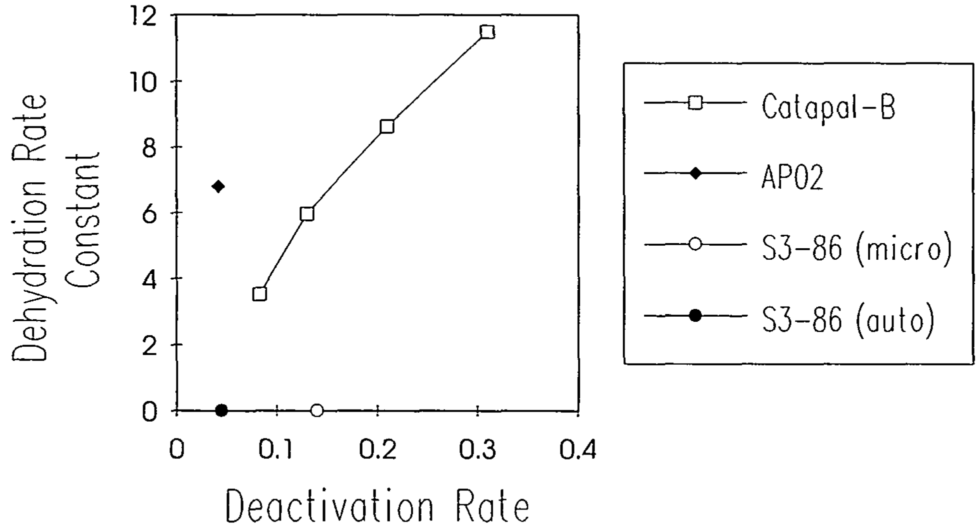

Figure 3.1.16 Arhennius Plot of LPDME™ Process Using S3-86 and Catapal-B

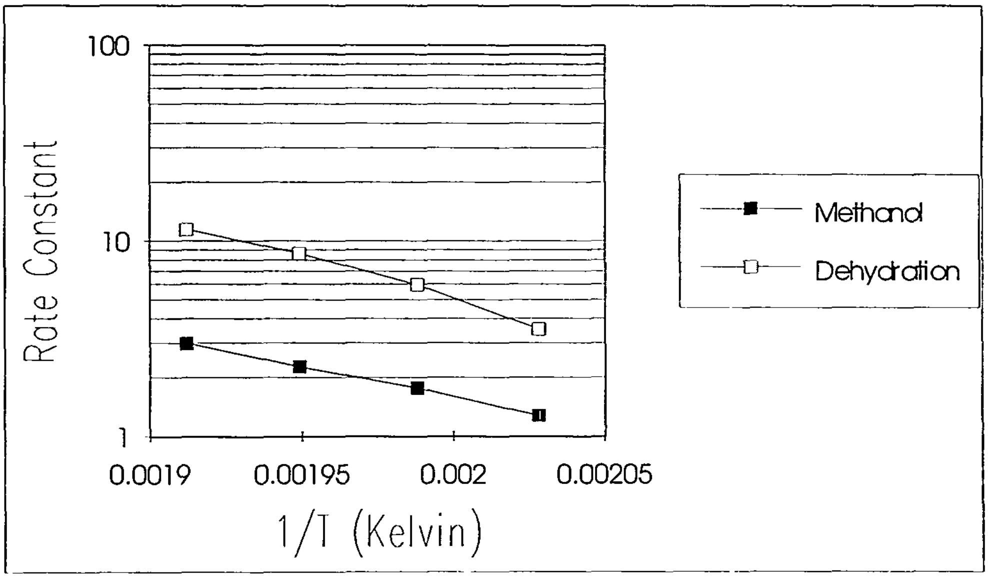

Task 3.2 New Fuels from Dimethyl Ether (DME)

Overall 2QFY96 Objectives

The following set of objectives appeared in Section III of Quarterly Technical Progress Report No. 5.

- Continue to screen immobilized catalyst candidates for hydrocarbonylation of dimethyl ether to ethylidene diacetate.
- Continue catalyst development work on the cracking of ethylidene diacetate to vinyl acetate and acetic acid.

Chemistry and Catalyst Development

(i) Dimethyl Ether (DME) to Ethylidene Diacetate (EDA)

This effort has focused on understanding the rhodium complexes anchored to the organic polymers for the catalytic conversion of DME to EDA and other single-step reactions that are involved in the overall DME to EDA net reaction.

Results and Discussion for Ionic Bound Rh to Polymer Catalyst

In previously reported work, the preparation of an ionically bound rhodium complex to a phosphinated Merrifield's resin was described. A series of experiments was performed to determine if there was leaching of rhodium from the resin during the catalytic runs. The experiments were conducted using a 300-cc reactor under the following conditions: acetic acid (69ml), methyl iodide (2ml), DME (5g), Merrifield's resin (0.45 g, containing ~ 5% Rh), 190°C, CO/H_2 (1:1, 1500psi) for 2 hours. The product was removed to a Whitey cylinder via a frit at the bottom of the reactor, leaving the catalyst in the reactor. The experiment was repeated with a fresh charge of reactants added to the reactor via the tube for the introduction of DME. After the reaction was repeated three times, there was a possibility that the catalyst was adhering to places in the reactor that the solution was not reaching. The reactor was therefore opened before the fourth run and rinsed with acetic acid, which was once again removed by the frit in the reactor, leaving the catalyst in the reactor. The reagents were then added as described above and the reaction was repeated. The results of the four experiments are shown in Table 3.2.1.

Table 3.2.1 Hydrocarbonylation of DME to EDA with Phosphine Catalyst

Experiment no	Conv. %	MeOAc Sel %	Ac_2O Sel %	EDA Sel%
1	98.9	46.4	9.5	20.5
2	98.2	51.8	12.5	17.9
3	97.5	63.6	9.3	9.4
4	97.8	42	5.9	5.8

The results show that the catalytic activity of the resin decreased from experiment 1 to 3. The methyl acetate concentration was observed to build up while the EDA conversion decreased. Between experiments 3 and 4, the reactor was washed with acetic acid, causing the product stream to be diluted and leading to a lower calculated selectivity for methyl acetate. Supporting this logic is that the methyl iodide concentration was also observed to be lower than the three previous runs, and the acetic acid concentration was higher. The conclusion from these experiments is that EDA selectivity did decrease for each run. This may have resulted from leaching of rhodium from the catalyst due to the inherent instability of resin at these temperatures. The solutions recovered from each run are being analyzed for rhodium, as is the recovered catalyst.

New Catalysts for DME to EDA Conversion

Thus far all the examples described involve anionically bound rhodium to a cationic polymer. In order to broaden our range of materials, it was decided to examine cationic rhodium complexes as catalysts. The complex $[Rh(dppe)_2]^+Cl^-$, dppe = diphenylphosphinoethane has been reported as an efficient catalyst for the gas phase carbonylation of methyl acetate to acetic anhydride. The complex was prepared according to the following procedure:

$$\underline{RhCl_3 + C_8H_{14} \longrightarrow [RhCl(C_8H_{14})_2]_2}$$

$$\underline{[RhCl(C_8H_{14})_2]_2 + 4\ dppe \longrightarrow [Rh(dppe)_2]^+Cl^-}$$

The product was characterized by its UV/VIS spectrum. The catalyst was tested as a homogeneous catalyst for DME to EDA conversion using the following procedure:

O.2g of catalyst, acetic acid (69ml), methyl iodide (2ml), DME (5g), 190°C, CO/H_2 (1:1, 1500psi) for 2 hours.

Analysis of the product showed a 90% DME conversion; however, the selectivity was 76% methyl acetate and only 2.5% acetic anhydride and EDA. This shows that the catalyst has low activity in the hydrocarbonylation reaction.

Methyl Acetate to Acetic Anhydride Heterogeneous Phosphine Catalyst versus Reillex Catalyst

Comparative experiments were conducted to broaden the utility of the anionic type polymeric catalysts. For the carbonylation of methyl acetate to acetic anhydride, the phosphinated heterogeneous catalyst was compared with the Reillex and homogeneous catalysts. The procedure and results are shown below and in Table 3.2.2:

300-cc reactor, MeOAc (0.695mol), CH_3I (0.074 mol), HOAc (0.29 mol), catalyst (0.8g), CO/H_2 (95/5), 190°C, 750psi. Analysis after 4 h.

Table 3.2.2 Carbonylation of Methyl Acetate to Acetic Anhydride		
Catalyst	MeOAc Conv %	Ac_2O Turnover Frequency (hr-1)
Phosphine 5.4 % Rh	34	122
Recycle	37	141
Reillex 2.24% Rh	45	159
Reillex 5.1%	36.5	110
Homogeneous, no LiI	30	99
Homo, with LiI	77	332

Table 3.2.2 shows that for the carbonylation of methyl acetate to acetic anhydride, the turnover frequency of the phosphinated catalyst is slightly better than the heterogeneous catalyst at comparable Rh loadings (122 vs 110). Both catalytic systems are better than the homogeneous system without LiI (turnover freq = 99). However, the homogeneous system with the LiI is still the best (turnover freq = 332).

Hydrogenation of Acetic Anhydride: Reillex vs Homogeneous

The hydrogenation of acetic anhydride to EDA was also studied, and the results are shown in Table 3.2.3. The experimental procedure is the following:

300-cc reactor, Ac_2O (0.22 mol), AcOH (2.4 mol), $RhCl_3.3H_2O$ (0.76mmol), LiI (0.1mol), LiOAc (7.8mmol), CH_3I (0.063mol), CO/H_2 (1:1), 190°C, 1500 psi, 2 hours.

Table 3.2.3 Hydrogenation of Acetic Anhydride to EDA				
Catalyst	Ac_2O Conv %	EDA Sel %	Turnover Frequency (hr^{-1})	Mass Bal. %
homo	85	47	29	72
hetero*	60	64	59	87
homo, no Li salts	58.8	17.5	7	62
hetero, no CH_3I	1	100	0.8	100

*Heterogeneous---use 1.8g of Reillex polymer containing 2.24% Rh by weight

The results show that the Reillex catalyst is still best for the hydrogenation of acetic anhydride. The presence of Li salts is essential for the homogeneous reaction to proceed and to a greater extent than in the carbonylation of methyl acetate. Methyl iodide was found to be necessary even for the heterogeneous reaction to proceed.

Recycle Experiments for DME to EDA using Heterogeneous Catalysts

In previous recycle experiments the assumption was made that if the rhodium leaches from the catalyst, the EDA concentration at a particular time will decrease with each successive run. This assumption was tested by performing catalytic runs with different amounts of catalyst and then determining if the response of EDA is linear or not.

The results in Figure 3.2.1 show that our assumption that the EDA concentration will increase as a function of the amount of rhodium present is a valid one. However, the graph shows that the amount of acetic anhydride at any one time cannot be correlated with the amount of rhodium.

Figure 3.2.1 Concentration Profile at 2 Hours versus Amount of Catalyst

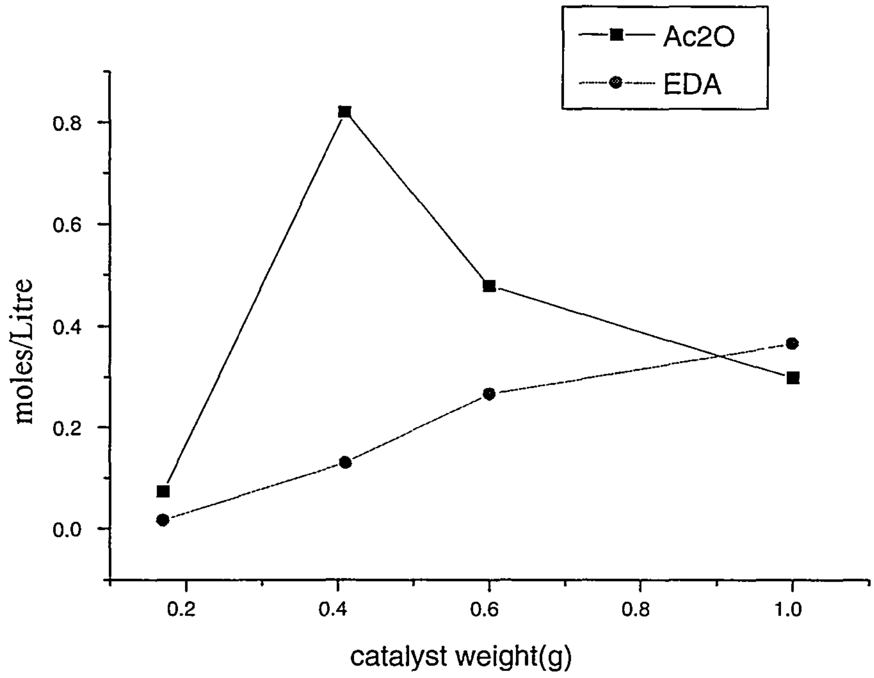

The recycling experiments were performed as follows. In a 300-cc autoclave, acetic acid (1.2 mol), DME (0.12 mol), methyl iodide (0.03 mol), and catalyst (phosphinated or Reillex) were added. The contents were pressurized with CO/H2 (1:1) at 1500psi at 190°C for two hours. The products were removed via a frit, and the catalyst was left in the reactor. The product concentrations were determined via GC, and the solutions were analyzed for rhodium. The experiment was repeated three times; the catalyst was recovered and analyzed for rhodium. The results of the experiments are shown in the Tables 3.2.4 and 3.2.5.

Table 3.2.4 Recycle Experiments for DME to EDA Using Heterogeneous Phosphine Catalyst

Exp. No	Conv%	MeOAc % sel	Ac_2O % sel	EDA % sel
1	98.9	46.4	9.5	20.5
Recycle	98.2	51.9	12.5	17.9
Recycle	97.5	63.6	9.28	9.35
Recycle*	97.8	42	5.9	5.8

*Mass balances ~ 85% for all except last recycle

Table 3.2.5 Recycle Experiments for DME to EDA Using Heterogeneous Reillex Catalyst

Exp. No	Conv%	MeOAc % sel	Ac_2O % sel	EDA % sel
1	99.1	16.9	19.5	47.6
Recycle	99.3	15.2	9.6	49.5
Recycle	99.3	9.2	26.4	46.8
Recycle*	99.4	9.2	20	46.8

*Mass balances in eighties for all runs

The results clearly show that the Reillex catalyst is a much better performer than the phosphinated heterogeneous catalyst in terms of selectivity to EDA. The Reillex catalyst decreased from 47.6% to 46.8% EDA selectivity by the third recycle, which was only a 1.5% loss. One could even make the case that this was within experimental error. The elemental analysis of the Reillex catalyst before the run was 2.56% Rh, and the recovered catalyst gave 2.26% Rh. Normally, we would expect a drop in this number after a run due to incorporation of methyl iodide in the polymer. However, if we assume that this is due to a loss of rhodium, then this amounts to a 11% loss based on initial Rh content. We should then have seen at least a 20% loss in EDA selectivity based on the graph showing concentration of EDA versus amount of catalyst. Since there is not such a large loss in activity for the Reillex material, it could be concluded that the elemental analysis of the Reillex was lower in rhodium after the run because of the incorporation of methyl iodide in the polymer. The elemental analyses of the recovered solutions did not support or disprove this point for the following reasons. If we assume the rhodium leached into the solution, this would give a value of 10 ppm in solution. The detection limit for the technique used was 50 ppm, and so a conclusive answer could not be obtained.

The selectivity towards EDA decreased from 20.5 to 5.8% by the third recycle for the phosphinated catalyst, which is a 72% loss in activity based on initial selectivity. The elemental analysis of the catalyst before the run was 6.6% Rh, and after the run it was 5.23% Rh. As discussed previously, we would expect a drop in Rh content due to methyl iodide incorporation in the polymer. However, if we assume loss of rhodium from the polymer due to leaching, this amounts to a 21% loss of Rh based on initial value. It seems unlikely that this would lead to such a dramatic loss in EDA selectivity (i.e.,72%). It is more likely that the catalyst is itself unstable in the hydrogen atmosphere, leading to a major loss in activity. Once again, the analysis of the recovered solutions did not support or disprove this point because the detection limit is 50ppm Rh, and we calculated the solution to have a maximum of 20 ppm Rh.

Based on the data we have obtained, the Reillex polymer is the best catalyst for DME to EDA conversion. A long-term stability test is planned for this catalyst. The analysis of the solutions for rhodium proved to be difficult due to the detection limits. We are planning to concentrate these solutions and repeat the analyses. One possible solution to this problem might be to prepare the catalyst in the reactor, and then analyze it for rhodium. After a few recycles, the rhodium content should not decrease due to methyl iodide incorporation, as this was done in the first step. If a significant loss is not seen, then leaching of Rh is not a problem.

(ii) Ethylidene Diacetate to Vinyl Acetate

Background for EDA Cracking

Ethylidene diacetate (EDA) {$CH_3CH(O_2CCH_3)_2$} can be cracked to vinyl acetate (VAM) {$CH_2{=}CHO_2CCH_3$} and acetic acid (AcOH) {CH_3CO_2H}. Ethylidene diacetate also reacts to yield acetic anhydride (Ac_2O) {$(CH_3CO)_2O$} and acetaldehyde (AcH) {$CH_3C(O)H$}. Reaction 1 depicts this series.

$$\mathrm{Ac2O + AcH} \longleftrightarrow \mathrm{EDA} \longleftrightarrow \mathrm{VAM + AcOH} \qquad \text{Rxn. 1}$$

In the last report, results of distillation cracking were discussed using iodide salts, particularly LiI. LiI was shown to crack EDA to VAM. LiI also catalyzed the retro-reaction to acetic anhydride and acetaldehyde. Several other lithium salts and several iodides were shown to be inactive.

Working from the assumption that the catalyst must be an iodide with a small cation, several additional materials were examined.

HI (Hydrogen Iodide)

In order to generate HI in situ, 1.75g of 57 wt % HI solution were reacted with 4.25g of acetic anhydride. This creates 1g of HI in 5g of acetic acid. The HI was then added to EDA and distilled at atmospheric pressure. VAM was observed in the distillate. However, the VAM peak was observed to disappear over the course of several injections. HI appears to cause further reaction of the VAM.

Ammonosorb Carbon

A 1g sample of Ammonosorb Activated Carbon was loaded with 20g of EDA and distilled at atmospheric pressure. The quaternary salt was soluble in the EDA, but yielded no reaction.

Calcium Iodide

A 1g sample of CaI_2 was loaded with 20g EDA and distilled.. A small amount of cracking to VAM was observed. Selectivity to VAM was only 4%. Retro-reaction was observed.

Iodine

A 1g sample of I_2 was tested as a catalyst. VAM was observed, but disappeared over time, as in the HI case.

Zinc Iodide

Based upon the known acidity of Zn ions, this material was tested. VAM was observed in the distillate. However, this material was very effective at catalyzing the retro-reaction, yielding acetaldehyde and acetic anhydride. Additionally, acetone was observed in the distillate.

Attempts to control the chemistry by addition of acetic anhydride were unsuccessful. Acetone, as well as a peak consistent with DME, was observed.

Lithium Iodide

The cracking of EDA with LiI was reported last time. In order to suppress retro-reaction, the experiment was repeated using a 5:1 molar ratio of acetic anhydride to EDA. The acetic anhydride was effective at reducing the production of acetaldehyde via the retro-reaction. Unfortunately, the catalyst activity was lowered significantly as well. Conversion dropped from 20 to 10%, selectivity was increased slightly to 50%, and the turnover was reduced from 30 to 4.

Magnesium Iodide

Based upon ionic radii, Li^+ and Mg^{++} are very similar. The higher charge may help to increase solubility. With this in mind, MgI_2 was examined as a cracking catalyst.

A 1g sample of MgI_2 was loaded with 20g of EDA and distilled at atmospheric pressure. VAM was observed in the distillate. Retro-chemistry was also observed. MgI_2 had a conversion of 51% with 27% selectivity to VAM. Turnover was calculated at 98.

The same material was tested with a feed consisting of 5:1 molar ratio of Ac_2O:EDA as described previously. Conversion of EDA was up slightly to 59%, while selectivity to VAM was 78%. Turnover dropped from 98 to 73.

The effect of higher acetic anhydride ratios is being explored.

Analytical Results

When performing many of the distillations described in these reports, we observed a low boiling fraction in the 35°C range. This fraction consisted of three components. The first two were assumed to be acetaldehyde and vinyl acetate based upon their retention times in the GC. The third material was tentatively identified as 3-acetoxy-2-butanone.

NMR has confirmed the GC data for acetaldehyde and vinyl acetate. The third component was identified as metaldehyde. Metaldehyde is a cyclic trimer of acetaldehyde. This finding is consistent with the appearance of this peak only when acetaldehyde is a principal component. Previous work on suppressing acetaldehyde formation by addition of acetic anhydride also caused suppression of this unidentified peak.

3QFY96 Objectives

Future plans for Task 3.2 will focus on the following areas:

- Continue to screen immobilized catalyst candidates for hydrocarbonylation of dimethyl ether to ethylidene diacetate
- Continue catalyst development work on the cracking of ethylidene diacetate to vinyl acetate and acetic acid.

Value Added Acetyls From Syngas (Eastman Chemical Company)

A. Introduction

The overall objective of this project is to produce a commercially viable process for the generation of vinyl acetate monomer (VAM) based entirely upon coal-generated syngas. Previous attempts at this objective have generally involved the combination of acetic anhydride (generated by carbonylation of either dimethyl ether or methyl acetate) with acetaldehyde (generated by either hydrogenation of acetic anhydride (Ac_2O) or hydrocarbonylation of either methanol (MeOH) or a methyl ester) to generate ethylidene diacetate (EDA), which is subsequently cracked to form VAM in a separate step. An exemplary process is shown below.

$$\begin{aligned}
2\,\mathrm{CO} + 4\,\mathrm{H_2} &\longrightarrow 2\,\mathrm{MeOH} \\
2\,\mathrm{MeOH} + 2\,\mathrm{AcOH} &\longrightarrow 2\,\mathrm{AcOMe} + 2\,\mathrm{H_2O} \\
\mathrm{AcOMe} + \mathrm{CO} + \mathrm{H_2} &\longrightarrow \mathrm{AcH} + \mathrm{AcOH} \\
\mathrm{AcOMe} + \mathrm{CO} &\longrightarrow \mathrm{Ac_2O} \\
\mathrm{Ac_2O} + \mathrm{AcH} &\longrightarrow \mathrm{EDA} \\
\mathrm{EDA} &\longrightarrow \mathrm{VAM} + \mathrm{AcOH}
\end{aligned}$$

AcH = acetaldehyde
AcOMe = methyl acetate

These efforts have failed to generate a commercially viable process to date. One of the key reasons for this failure was the very large quantities of recycled acetic acid (and consequently large commercial facilities) inherent in the earlier proposed processes.

Eastman's proposal was to circumvent the recycle problem by generating AcH via hydrogenation of acetic acid (AcOH) instead of via reductive carbonylation. Unfortunately, this process is thermodynamically disfavored and, even if acetic acid is hydrogenated, the conditions required generally favor further hydrogenation to form ethanol and ethyl acetate, which are the thermodynamically favored products. Currently, any processes that have successfully hydrogenated a carboxylic acid circumvent this problem by operating at unacceptably high pressures and temperatures to overcome the thermodynamic constrictions and by operating at low conversion to minimize over-hydrogenation to the alcohol.

Eastman's proposed solution to this dilemma was to convert the acetic acid to ketene (a very well known process) and utilize the high energy content of the unstable ketene intermediate to overcome the thermodynamic constrictions to hydrogenation. The key task would be to identify catalysts that hydrogenated the ketene intermediate selectively to acetaldehyde (particularly did not generate ethanol or ethyl acetate) and would do so at commercially desirable temperatures and pressures.

Several restrictions are inherent in the contemplated conversion. Due to the unstable nature of ketene, the vapor pressure of ketene in the process should be less than atmospheric and its conversion should be reasonably high. Further, recovery of acetaldehyde will require that there not be excessive amounts of additional hydrogen present. Prior to this study, no catalyst was known for accomplishing this task.

Whereas the hydrogenation of acetic acid represents the linchpin technology in the proposal, also included were some proposed advances in the subsequent conversion of acetaldehyde to VAM. Obviously, the acetaldehyde thus formed could be converted to EDA and subsequently to VAM by known methods; Eastman proposed several improvements upon this known process. However, Eastman also proposed a very speculative application of ketene for the direct esterification of acetaldehyde to yield VAM without the intermediate generation of significant amounts of EDA. If this overall speculative conversion came to fruition, the process would be represented by the following relatively simple scheme:

Scheme 1. Conversion of Syngas to VAM from Acetic Acid via Ketene

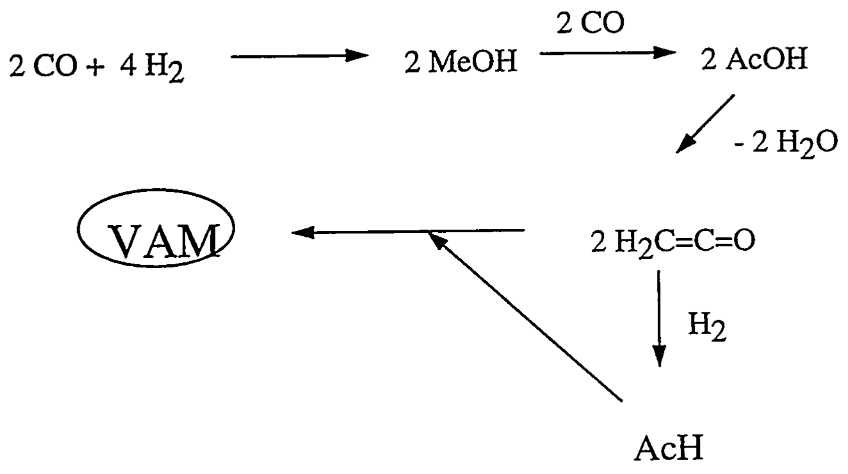

It is particularly important to point out that this scheme does not have any significant recycle loops. Further, due to the nature of the process, there are numerous opportunities to reduce capital costs through proper integration, and there is a notable economy of scale associated with the size of the intermediate steps.

Consistent with these goals, Eastman has pursued the following tasks in the 1st quarter of 1996:

Task 1.1. Examine hydrogenation of AcOH to acetaldehyde via ketene.
Task 2.1. Examine the direct conversion of AcH and ketene to VAM.
Task 3.1.a. Assess preliminary economics for a process based on ketene hydrogenation.

In addition, Eastman has begun to reconsider the role reductive carbonylation of methanol (or its derivatives) might play in this process as a means of generating acetaldehyde for the process, given the success of Task 2.1.

B. Results and Discussion

General. Eastman is now operating three reactors. The two smaller scale reactors are set up to separately investigate hydrogenation (particularly heterogeneous hydrogenation) of ketene, and the gas stripped reactor is designed for the direct conversion of ketene and acetaldehyde to VAM. The larger scale reactor (0.6-0.8 moles/hr) is set up to be more flexible in its operation and should be useful in examining scaleup or alternative reactor designs for either conversion.

Task 1.1. Hydrogenation of AcOH via Ketene Intermediates. In its previous report, Eastman described a series of Pd-based catalysts for the hydrogenation of ketene to acetaldehyde. Within the report, Eastman described a procedure that isolated ketene at dry ice temperatures and then slowly metered ketene into the hydrogenation unit using a stream of nitrogen nearly saturated in ketene. Although these runs were successful, Eastman sought to scale up the process and eliminate the large volume of diluent gas associated with this method of introduction.

To do this Eastman constructed two continuous ketene generators that utilized acetone as a source of ketene. (One of these units represented a scaleup factor of ca. 10 over its previous units.) A ketene generation rate was established for each and, using the smaller reactor, a continuous feed of freshly generated, undiluted ketene was introduced to the hydrogenation reactor.

The catalyst deactivated rapidly with the freshly generated, undiluted ketene feed. However, this deactivation was readily reversible by simply cutting off the ketene feed (while maintaining the hydrogen feed) for a period of time. After reactivation, catalyst activity (measured by the older method of ketene introduction) was virtually the same as the original catalyst. The likely cause of this deactivation was carbon monoxide, which is an inevitable consequence of ketene generation. (Generally, 1-3% of the feed to a ketene reactor is lost to the formation of CO.) In the earlier experiments, Eastman separated the ketene from the carbon monoxide co-product by condensation at dry ice temperatures and, therefore, this mode of deactivation was not operable.

This observation has several important ramifications. If the catalyst is to be used as it currently exists, the hydrogenation must be conducted either using two reactors (one is undergoing reactivation while the other is in use) or by utilizing a cryogenic separation of ketene. Neither is as desirable as identifying a CO-tolerant catalyst.

The advent of a CO-tolerant catalyst would simplify the process, but would also cut costs by allowing the use of less pure hydrogen (i.e., allow some carbon monoxide content). Eastman will be devoting significant efforts to identifying a CO-tolerant catalyst in the near future and has envisioned a host of candidates from classical homogeneous and heterogeneous catalysts with which the presence of CO might actually be advantageous. (A final alternative that will not be discussed in detail at this time is the use of a CO absorbing unit.)

In the interim, Eastman has designed and constructed a bench-scale unit that allows the continuous cryogenic separation of ketene from the CO impurity, as well as any other non-condensable gases. This unit, which is depicted in Figure 3.2.2, has been used to demonstrate hydrogenation at higher feed rates in the absence of significant diluents. The unit is fairly new, and its usefulness, while demonstrated, has not yet been completely exploited. As demonstrated by the comparison shown below, the unit has been used to successfully examine the hydrogenation of ketene in the absence of diluent gases; a comparison is made between undiluted feeds using the cryogenic separator and previous runs in the presence of copious quantities of diluent gas.

Ketene Hydrogenation Experiments

Hydrogenation with Undiluted Feed:

Conditions:

- 0.633 mmol ketene/minute
- 2.0 mmol H_2/minute
- 1.001 g (2.6 mL) 5% Pd/C catalyst
- 98°C
- Space velocity = 1850 hr^{-1}

Results:

- HAc space time yield = 495 $g\text{-}L^{-1}\text{-}hr^{-1}$
- Ketene conversion = 77 %
- Ketene accountability = 100 %
- HAc selectivity = 100 %

Hydrogenation with Diluted Feed Evaluated Previously:

Conditions:

- 1.0 mmol ketene/minute
- 2.0 mmol H_2/minute
- 6.2 mmol He+N_2/minute
- 1.003 g (2.6 mL) 5% Pd/C catalyst
- 98°C
- Space velocity = 6400 hr^{-1}

Results:

HAc space time yield = 610 g-L^{-1}-hr^{-1}
Ketene conversion = 100 %
Ketene accountability = 60 %
HAc selectivity = 60 %

Figure 3.2.2 Continuous Benchscale Cryogenic Separator for Ketene

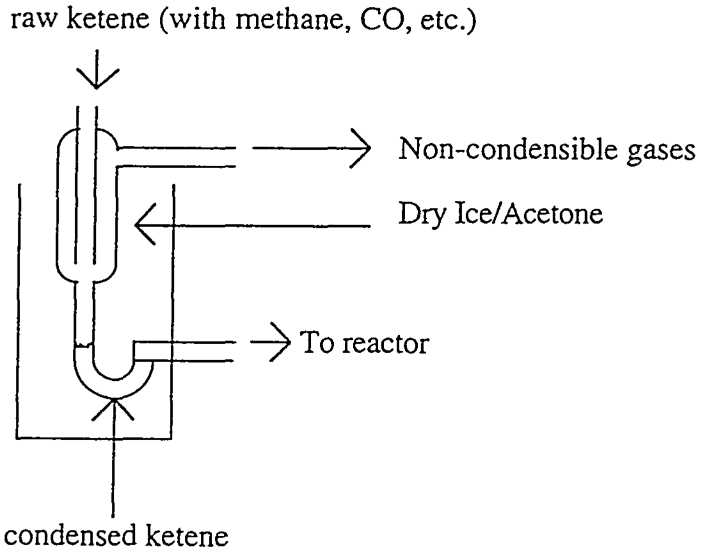

Task 2.1. Direct Conversion of Ketene and Acetaldehyde to VAM. Although methods existed for the conversion of acetaldehyde and syngas-derived acetic anhydride to VAM, Eastman perceived a potential advantage to using the ketene directly for the conversion of acetaldehyde to vinyl acetate. Traditionally, the conversion was carried out by mixing acetic anhydride and acetaldehyde and isolating the vinyl acetate from the equilibrium mixture (represented by the two equations shown below), even though the equilibria favored EDA formation.

$$Ac_2O + AcH \rightleftharpoons EDA \qquad K_{140°C} = 25$$

$$EDA \rightleftharpoons VAM + AcOH \qquad K_{140°C} = 0.01$$

Eastman envisioned this addition as a means to consume the AcOH *in situ* by reaction of ketene as follows:

$$H_2C{=}C{=}O + AcOH \longrightarrow Ac_2O$$

At the operating temperatures of this reaction (<140°C), the reaction would be essentially irreversible, and the process should be driven toward the generation of previously disfavored vinyl acetate by the continuous consumption of acetic acid. This process not only has the potential advantage of improving the efficiency of VAM formation, but would replace the acetic anhydride generation facility in earlier concepts with a simplified acetic acid process. (Purity requirements for ketene generation are much less strict than for other acetic acid applications.)

In the previous quarterly, Eastman reported the initial demonstration of this significant advance in VAM generation using a gas stripped reactor, such as the one diagrammed in Figure 3.2.3. Over the last quarter, Eastman examined a number of additional catalysts and conditions for this conversion using this gas stripped reactor. As can be seen from the results below, the optimal catalysts are aromatic sulfonic acids and the optimal solvent is acetic anhydride.

Figure 3.2.3 Gas Stripped Reactor for Direct Conversion of Ketene and Acetaldehyde to Vinyl Acetate

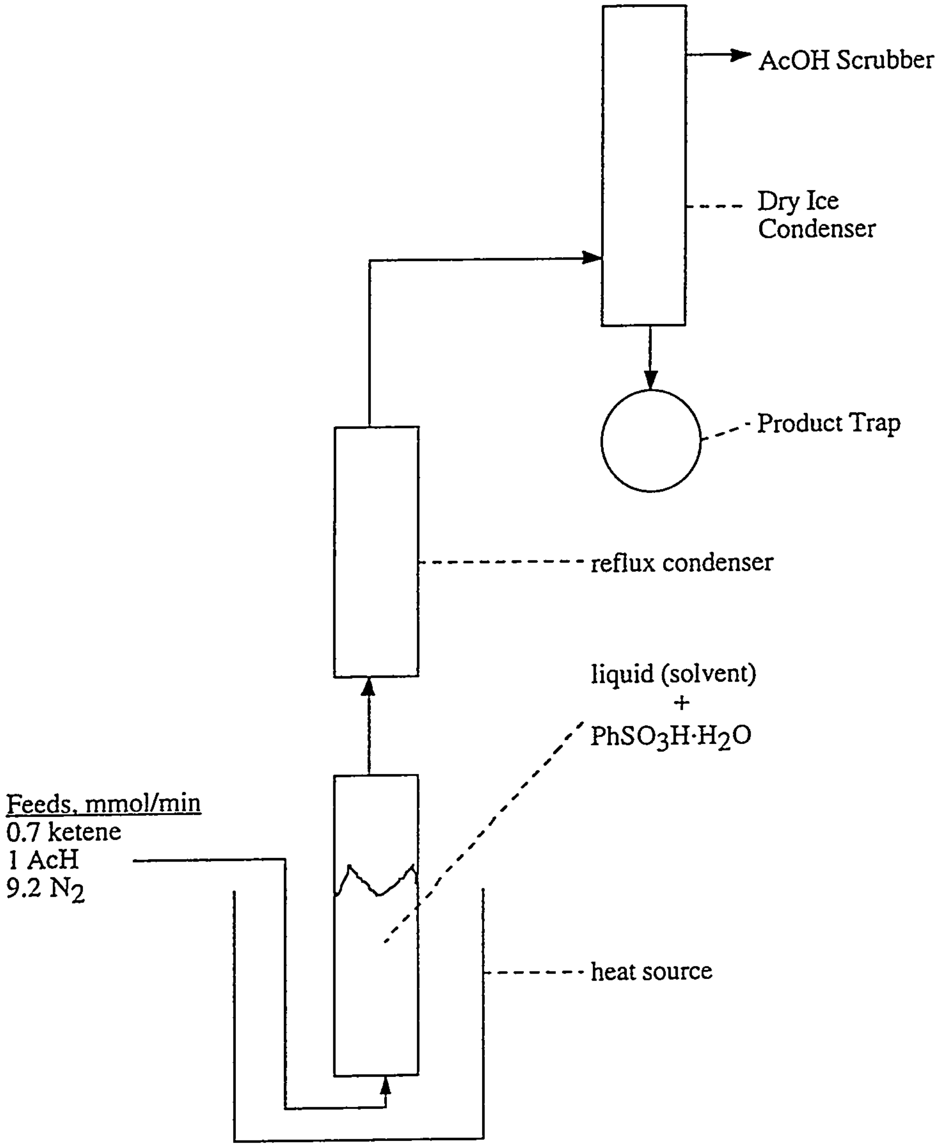

Results for Task 2.1.

A. Gas Stripped Reactor for The Production of VAM

1. Arene Sulfonic Acids

a) Acetic Anhydride as Solvent

Conditions:
30.6 mmol arenesulfonic acid.H_2O
61.6 mmol acetic acid
583 mmol acetic anhydride
0.7 mmol ketene/minute
1.0 mmol acetaldehyde/minute
9.2 mmol N_2/minute
150°C
Run 5-6 hours per day for 1 to 4 days

1) *Results with benzenesulfonic acid*
VAM yield from ketene:
1st day = 50%
2nd day = 90%
3rd day = 92%
4th day = 78%

Accountability for the whole run:
ketene = 107%
acetaldehyde = 106%

2) *Results with p-toluenesulfonic acid*
VAM yield from ketene:
1st day = 41%
2nd day = 86%
3rd day = 95%
4th day = 87%
Accountability for the whole run:
ketene = 119%
acetaldehyde = 114%

NMR of trap material of 4th day:
60.9% VAM
36.7% acetaldehyde
2.4% acetic anhydride,
no acetic acid or any other species

Can account for the components of 80.1 g of the 80.6 g heel (diff. 0.5 g).
Heel contained 35.7 wt % EDA.